



# Extrapolation of anthropogenic disturbances on hazard elements in PM<sub>2.5</sub> in a typical heavy industrial city in northwest China

Bianhong Zhou<sup>1,2</sup> · Jin Wang<sup>1</sup> · Suixin Liu<sup>2,4,5</sup> · Steven Sai Hang Ho<sup>3</sup> · Tingting Wu<sup>2</sup> · Yong Zhang<sup>2</sup> · Jie Tian<sup>2</sup> · Qiao Feng<sup>1</sup> · Chunyan Li<sup>1</sup> · Qiyuan Wang<sup>2,4,5</sup>

Received: 7 January 2022 / Accepted: 6 April 2022 / Published online: 26 April 2022  
© The Author(s), under exclusive licence to Springer-Verlag GmbH Germany, part of Springer Nature 2022

## Abstract

Baoji is a typical heavy industrial city in northwest China. Its air quality is greatly impacted by the emission from the factories. Elements in fine particulate matter (PM<sub>2.5</sub>) that are greatly emitted from anthropogenic sources could pose diverse health impacts on humans. In this study, an online AMMS-100 atmospheric heavy metal analyzer was used to quantify 30 elements in PM<sub>2.5</sub> under the weak and strong anthropogenic disturbance scenarios before the city lockdown period (from January 9<sup>th</sup> to 23<sup>rd</sup>) and the lockdown period (from January 26<sup>th</sup> to February 9<sup>th</sup>) due to the outbreak of COVID-19 in 2020. During the lockdown period, the average total concentration of total quantified elements was 3475.0 ng/m<sup>3</sup>, which was 28% and 33% lower than that of the weak and strong anthropogenic disturbance scenarios during the pre-lockdown period. The greatest reductions were found for the elements of chromium (Cr), titanium (Ti), manganese (Mn), and Zinc (Zn), consistent with the industrial structure of Baoji. The mass concentrations of most elements showed obvious reductions when the government post-alerted the industries to reduce the operations and production. Dust, traffic sources, combustion, non-ferrous metal processing, and Ti-related industrial processing that are the contributors of the elements in the pre-lockdown period were apportioned by the positive matrix factorization (PMF) model. Substantial changes in the quantified elements' compositions and sources were found in the lockdown period. Health assessment was conducted and characterized by apportioned sources. The highest non-carcinogenic risk (HQ) was seen for Zn, demonstrating the high emissions from the related industrial activities. The concentration level of arsenic (As) exceeded the incremental lifetime carcinogenic risk (ILCR) in the lockdown period. This could be attributed to the traditional firework activities for the celebration of the Chinese New Year within the lockdown period.

**Keywords** Disturbances · COVID-19 · Elements · Industry · Firework · Health assessment

Responsible Editor: Constantini Samara

✉ Qiyuan Wang  
wangqy@ieecas.cn

- <sup>1</sup> Shaanxi Key Laboratory of Disaster Monitoring and Mechanism Simulation, College of Geography & Environment, Baoji University of Arts & Sciences, Baoji 721013, China
- <sup>2</sup> State Key Laboratory of Loess and Quaternary Geology, Institute of Earth Environment, Chinese Academy of Sciences, Xi'an 710061, China
- <sup>3</sup> Division of Atmospheric Sciences, Desert Research Institute, Reno, NV 89512, USA
- <sup>4</sup> CAS Center for Excellence in Quaternary Science and Global Change, Xi'an 710061, China
- <sup>5</sup> Shaanxi Key Laboratory of Atmospheric and Haze-fog Pollution Prevention, Xi'an 710061, China

## Introduction

PM<sub>2.5</sub>, particulate matter with an aerodynamic diameter of less than 2.5 micrometers, is an important component for air quality assessment. It is necessary to understand its chemical compositions and their associated roles in atmospheric chemistry. PM<sub>2.5</sub> mainly consists of inorganic ions, elements, and organic constituents (Yin et al. 2019). Even though elements occupy relatively small mass proportions in PM<sub>2.5</sub>, they pose great harm to human health. For example, vanadium (V) and chromium (Cr) play a key role to induce the oxidization of DNA, and exposure to high concentrations of arsenic (As) can damage the nervous system (Tenías et al. 2010). The elements of Cr, cadmium (Cd), cobalt (Co), mercury (Hg), nickel (Ni), lead (Pb), and selenium (Se) are listed as carcinogens by the United States Agency for

Toxicology and Disease Registry (ATSDR) (Sorensen et al. 2005; Thomas et al. 2009). Presently, elements in  $PM_{2.5}$  were mostly studied from the particle collections on the filter matrix and then analyzed by an X-ray fluorescence analyzer (XRF) (Han et al. 2015; Zhou et al. 2020), inductively coupled plasma mass spectrometer (ICP-MS) (Hwang et al. 2018; Hana et al. 2020), or atomic absorption spectrometer (AAS) (Shah et al. 2012). However, offline sampling has some disadvantages such as low time resolution, large manpower consumption, and delay in reporting analytical results from stepwise data processing. In comparison, the online measurement not only reduces these shortcomings but also effectively determines the correlations between the elemental concentrations and short-term changes in meteorological parameters and pollution sources. However, only limited studies have applied the online approach to quantify the particulate-bound elements. Wang et al. (2018) determined the concentration of 18 metals in  $PM_{2.5}$  using an ambient continuous multi-metals monitor. The minimum detection limits (MDLs) of elements ranged from 0.063 ng/m<sup>3</sup> for arsenic (As) down to 100 ng/m<sup>3</sup> for aluminum (Al). The instrument could automatically use three metals (i.e., Cr, Cd, and Pb) with a built-in probe for internal calibration each day and offer an allowable deviation range of 5%. Zhang et al. (2021) compared the 1 h time resolution data for 28 elements in  $PM_{2.5}$  in Tianjin, China, using an online heavy metal analyzer and the offline filter sampling coupled with the XRF analysis, respectively. They observed that the annual online means were higher than those of the offline data, but there was no solid conclusion on the discrepancy. Much possible explanation is the unavoidable loss of particles from the filter matrix during handling.

Baoji is a typical heavy industry city in northwest China with a long history. It has been at the leading position in gross production and is supported by governmental policies (Zhang 2004, 2007). In 2021, there are 224 industries, covering 35 industrial categories, while the numbers of industrial enterprises are more than 6200 households. In between, there are 795 enterprises above the designated size, and the total industrial output value of the city exceeds 300 billion yuan per year, with an annual growth rate of 15% (Li 2021). The main industries mainly include non-ferrous metal processing and smelting, auto parts processing, manufacturing of heavy-duty trucks, numerical control machine tools, petroleum equipment, and rail transportation. More than 60 products such as machine tools, steel pipes, and oil drilling equipment occupied the Chinese market. Specifically, the sales volume of titanium (Ti) products such as drilling equipment, computer numerical control machine tools, and other related products rank at the top of the industry in China. As a titanium valley, the output of titanium products accounts for 85% of the national market and even 22% of the world market (Zhang et al. 2021). However, there is still

a lack of awareness for the enterprises to develop an efficient governance system that controls and minimizes heavy metal pollution to the environment. In fact, the government has launched a local system to alert the pollution status for public health protection. When the system forecasts potential high pollution occurred, a warning would be given to the key industries, and the emission would be thus reduced under a series of an emergency plan. It is identified as a weak anthropogenic disturbance period. The other time is then defined as a strong anthropogenic disturbance period.

The intensities of human activities are typically proportional to anthropogenic pollution sources and the degrees of impact on the air quality. During the outbreak of COVID-19, most anthropogenic emission sources were greatly reduced (Wang et al. 2020; Nguyen et al. 2021). For an industrial dominated city, the pollutant emission from most industrial enterprises largely diminished during the lockdown period of COVID-19, providing a unique natural condition to identify the human disturbance on the air quality. Owing to the merits of using the online method, an online AMMS-100 atmospheric heavy metal analyzer has been used to acquire high-resolution element data. The objectives of this study are to (1) quantify the important elements in  $PM_{2.5}$  using the online method, (2) interpret and elaborate on the pollution sources and characteristics at different intensities of anthropogenic pollution in Baoji, and (3) conduct the health assessment and provide a relevant theoretical basis.

## Methodology

### Sampling site

The monitoring was conducted from January 9<sup>th</sup> to February 9<sup>th</sup>, 2020. According to the notice issued by the People's Government of Shaanxi Province (<http://www.shaanxi.gov.cn/>), the study period could be divided into two major stages, the pre-lockdown (January 9<sup>th</sup> to January 23<sup>rd</sup> 2020) and the lockdown (January 26<sup>th</sup> to February 9<sup>th</sup> 2020) with minimal anthropogenic, particularly industrial, and anthropogenic disturbances. The pre-lockdown could be further divided into strong anthropogenic disturbance (occurred in warning inactivated) and weak anthropogenic disturbance (occurred in warning activated) scenarios. Most anthropogenic and commercial activities were usual during the warning inactivated periods, but the activities of the industrial sector and vehicular usage were strongly regulated or forbidden when the warning was activated, according to documents released by the Shaanxi Province Government Office ([http://zjj.baoji.gov.cn/art/2020/1/9/art\\_2141\\_10252.html](http://zjj.baoji.gov.cn/art/2020/1/9/art_2141_10252.html), and [http://sthjj.baoji.gov.cn/art/2020/1/14/art\\_3678\\_477481.html](http://sthjj.baoji.gov.cn/art/2020/1/14/art_3678_477481.html), in Chinese) (Table 1).

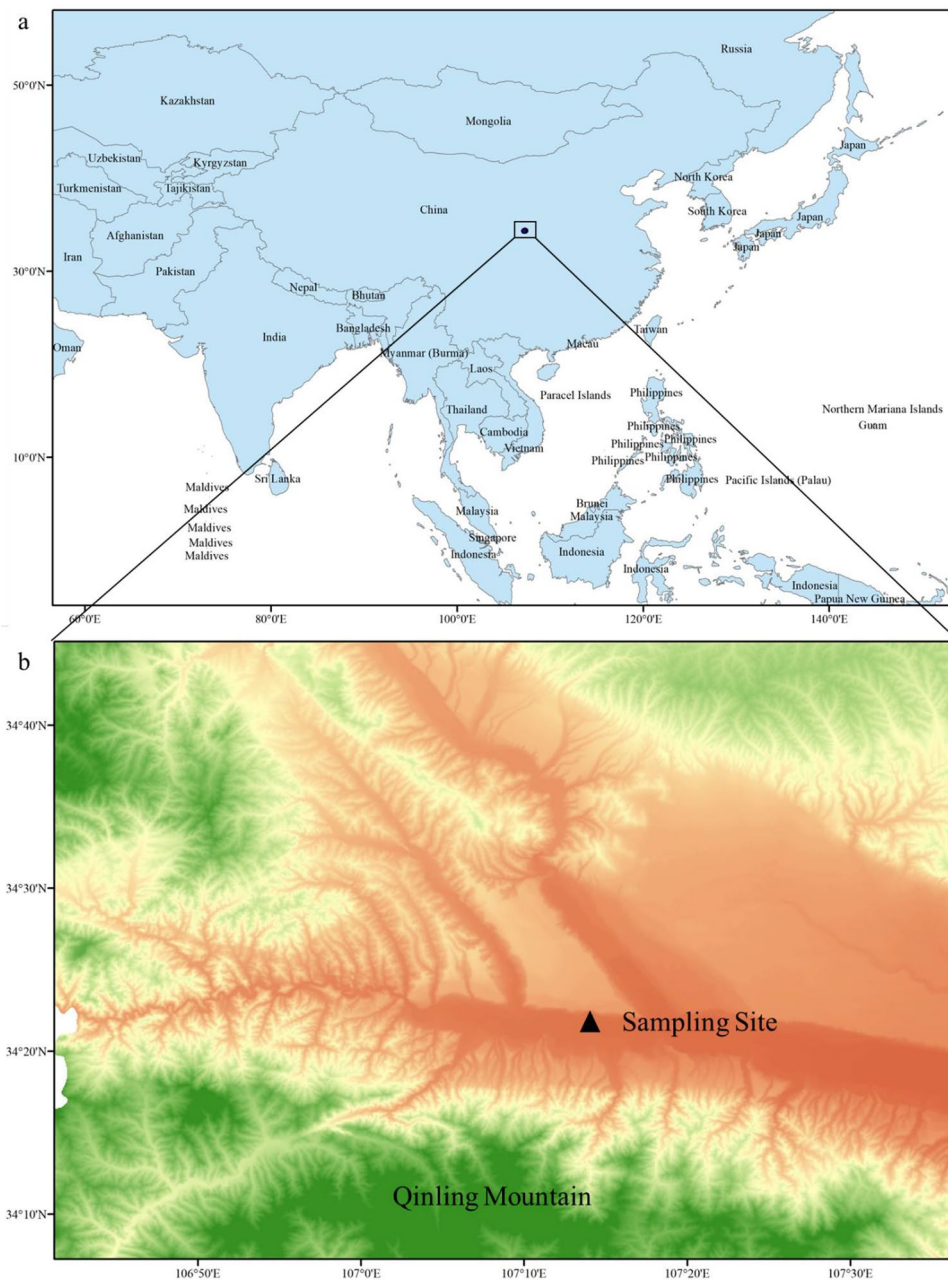
**Table 1** Warning hosted in the study year 2020

Date	Time (LT)	Warning
January 8th	18:00	Orange warning for heavy pollution
January 14 <sup>th</sup>	14:00	Orange warning has been lifted
January 17 <sup>th</sup>	10:00	Orange warning for heavy pollution
January 24 <sup>th</sup>	15:00	Orange warning has been lifted

The observation site is on the roof of a hotel (107°14'9"E, 34°21'29"N) in the Baoji High-tech Zone

(Fig. 1), ~100 m above the ground level. No building was found nearby. The Weihe River is to the north, adjacent to a commercial street in the south. The residential area is to the west, and the Panlong Bridge with a large traffic flow is 100 m to the east. Five industrial parks are in Baoji, including the Yongqing Industrial Park (~2.5 km to the southeast), the Baoji Titanium Industrial Park and Gaojiaya Village Industrial Park (~4 and ~5 km away, respectively), the Chenjiaya Industrial Park of Qianhe (7.8 km to the northwest), and the processing zone of the Baoji High-end Equipment Industrial Park (3.5 km to the southwest).

**Fig. 1** Maps of Baoji city in China (a) and the distribution of the five industrial parks nearby the sampling site (b)



### Instrumentation

The online AMMS-100 atmospheric heavy metal analyzer (Jvguang, Hangzhou, China) was used to determine the PM<sub>2.5</sub> bound elements. The instrument consists of five parts: sampling, motion, XRF, control, and remote transmission subsystems. The working principle is that the air is filtered, and the particles are enriched on the filter membrane by a sampling probe and a dust cutter at a flow rate of 16.7 L/min by a pump. The collection cycle is set to 1 h. Then, the filtration membrane moves to the analytical area by rotating on a conveyor. The particles on the filter membrane are determined with XRF technology for qualitative and quantitative analysis of the elements. A mass flowmeter is equipped to record the sampling volume. The next sample is collected at the same time while the previous sample is being analyzed.

Before the sampling campaign, flow calibration, blank filter band detection, and standard diaphragm calibration were performed according to the standard operation procedures (SOPs). To ensure the accuracy of the data, the filter membrane was changed, the sampling head and cutter were cleaned, and the airtightness of the instrument was checked regularly. A total of 30 elements were able to be quantified in this work. In this paper, fourteen elements (including Sc, Tl, Pd, Te, Cd, Co, Ga, Hg, Cs, Ni, Sb, Ag, Sn, and V) that had loadings at least 50% below their MDLs were excluded in our elaborations. The MDLs for the elements at a time resolution of 1 h ranged from 0.15 to 55.8 ng/m<sup>3</sup> (Table 2).

### Data analysis methods

#### Positive matrix factorization

Positive matrix factorization (PMF), first proposed by Paatero and Tapper (1994), is a method of particle source analysis based on the least square method. The largest advantage of this method is that, on the premise of unknown source spectral information, the source type can be inferred by combining the calculation and markers of the source, so it is widely used in gas source analytical research (Dai et al. 2020; Hao et al. 2018; Manousakas et al. 2017). PMF decomposed the data of sample concentration into factor contribution (*g*) and factor component spectrum (*f*) and identified factor quantity and factor contribution through the multi-linear multi-iteration algorithm (Liu et al. 2015). The formula is as follows.

$$X_{ij} = \sum_{k=1}^p g_{ik} f_{kj} + e_{ij} \tag{1}$$

where  $X_{ij}$  is the concentration of the *j* chemical component in the *i*th sample, and the unit is  $\mu\text{g}/\text{m}^3$ ;  $g_{ik}$  is the contribution of the *k*-type source in the *i*th sample, and the unit is  $\mu\text{g}/\text{m}^3$ ;  $f_{kj}$  is the mass percentage of the *j* chemical component in the *k* source; and  $e_{ij}$  is the residual of the *j* chemical component in the *i*th sample. The object function of the model is *Q*. The uncertainty  $u_{ij}$  and non-negative matrix elements  $g_{ik}$  and  $f_{kj}$  were given as the restriction conditions. *Q* can be further analyzed only when *Q* converges. The smaller value of *Q* is selected for multiple runs to continue the analysis, and the specific calculation is as follows.

$$Q = \sum_{i=1}^n \sum_{j=1}^m \left[ \frac{X_{ij} - \sum_{k=1}^p g_{ik} f_{kj}}{u_{ij}} \right]^2 \tag{2}$$

where  $u_{ij}$  represents the uncertainty of species *j* in sample *i*, and the uncertainty calculation method.

When the concentration of chemical components was less than the MDL, the uncertainty (Unc) was calculated as follows.

$$\text{Unc} = \frac{5}{6} \times \text{MDL} \tag{3}$$

When the concentration of chemical components was higher than MDL. Unc was calculated as below.

$$\text{Unc} = \sqrt{\text{Error Fraction} \times C^2 + (0.5 \times \text{MDL})^2} \tag{4}$$

Among them, the sampling and analysis time of the online analyzer is 60 min. MDL in this study is subject to 1 h. Error fraction refers to the error of each element, and the error of the online instrument was set to 10% (Chang et al. 2018). *C* refers to the measured concentration of each element.

The overall uncertainty of the model is usually set between 1% and 20%. According to the size of the element signal-to-noise ratio (S/N), select the data required for the actual simulation of the model. If  $S/N > 1$ , set it to “strong.” If  $1 \geq S/N \geq 0.5$ , set it to “weak.” If  $S/N < 0.5$ , set it to “bad.” In the output results, all values of Q(Robust) are close, which indicates that the model runs stably. All values of Q(True) are yes, and the Q(Robust)/Q(True) tends to 1, the higher the fitting degree is.

**Table 2** The MDLs for the elements accounted with a time resolution of 1 h (unit: ng/m<sup>3</sup>)

Element	Se	As	Br	Cr	Mn	Ca	Pb	Zn
MDL	0.07	0.15	0.16	0.16	0.19	0.22	0.23	0.29
Element	Ti	Mo	Ba	Cu	Fe	K	Si	Al
MDL	0.31	0.34	0.36	0.69	1.44	2.83	4.52	55.8

**Health risk assessment**

Health risk assessment is a health risk assessment model proposed by the United States Environmental Protection Agency (U.S.EPA. 2010), which is mainly used to calculate the harm degree of heavy metals to an adult male, adult female, and children. Life average daily dose (LADD) and average daily dose (ADD) of each heavy metal to a specific population are calculated as follows.

$$ADD = (c \times IR \times EF \times ED)/(BW \times AT) \tag{5}$$

$$LADD = (c \times IR \times EF \times ED)/(BW \times AT) \tag{6}$$

where *c* is element mass concentration, IR is respiration rate, EF is exposure frequency, ED is exposure years, BW is body weight, and AT is average exposure time. The calculation method of AT is different between non-carcinogenic and carcinogenic effects. For ADD, AT evaluates the non-carcinogenic harmful effects of pollutants according to the exposure cycle of the population. For LADD, AT considers the lifetime exposure hazards of the population, so the lifetime carcinogenic risk of pollutants is assessed according to the average life expectancy of the population (The Ministry of Environmental Protection 2013). Table 3 lists the parameter values for the calculations.

Non-carcinogenic risk (HQ) and carcinogenic risk (ILCR) through the respiratory pathway were calculated as below.

$$HQ = ADD/RFD \tag{7}$$

$$ILCR = LADD \times SF \tag{8}$$

where RFD is the reference dose, SF is the slope factor of cancer risk of elements by breathing, and the values of the

**Table 3** Exposure parameters used for different age groups

Parameter	Unit	Child	Male	Female
<i>c</i> <sup>a</sup>	mg/m <sup>3</sup>			
IR <sup>b</sup>	mg/d	8.6	16.6	13.5
EF <sup>c</sup>	d/a	365	365	365
ED <sup>d</sup>	a	6	30	30
BW <sup>e</sup>	kg	15	67.3	57.3
AT (non-carcinogenic) <sup>f</sup>	d	365×ED	365×ED	365×ED
AT (carcinogenic)	d	365×18	365×72.4	365×77.4

<sup>a</sup>*C* is concentration of element

<sup>b</sup>IR is respiratory rate

<sup>c</sup>EF is exposure frequency

<sup>d</sup>ED is exposed fixed number of years

<sup>e</sup>BW is weight

<sup>f</sup>AT is average exposure time

two factors are shown in Table 4. When  $HQ \leq 1$ , the non-carcinogenic health risk can be ignored. When  $HQ > 1$ , there is a non-carcinogenic risk. When  $ILCR < 10^{-6}$ , the carcinogenic risk could be ignored. When ILCR is between  $10^{-6}$  and  $10^{-4}$ , there is a certain risk of cancer. When  $ILCR > 10^{-4}$ , there is a higher risk of cancer.

**Results and discussions**

**Elemental pollution characteristics**

Table 5 lists the concentrations of elements measured in the two periods. The average mass concentration of the total quantified elements at the lockdown period was 3475 ng/m<sup>3</sup>, exhibiting a moderate reduction of 30.6% from the pre-lockdown period (5008 ng/m<sup>3</sup>). To verify the potential influences of meteorological factors on the elements, the evaluations were carried out with and without their considerations according to the circulation coefficient used by Mishra et al. (2021). The results showed that meteorological conditions had no obvious influence on the inorganic elements. Therefore, the influences of the meteorological factors were not considered in this study. However, few elements showed reverse observations. The abundance of elements K, Ba, and Br increased at the lockdown period. As known, K and Ba could be emitted by household fireworks for the traditional celebration during the Chinese Spring Festival (Rai et al. 2020; Yao et al. 2019). Except for K, Ba, and Br, the mass concentrations of other elements showed declines in the lockdown period. The largest reductions were seen for Cr, Ti, Mn, and Zn at 86.1%, 83.0%, 80.8%, and 77.6%, respectively, demonstrating that anthropogenic activities had a particularly great impact on these elements. Other elements declined at rates were >15%, possibly attributed to the city lockdown as well.

In terms of the degree of anthropogenic disturbances, the total quantified elements for the weak and strong disturbances scenarios during the pre-lockdown period were

**Table 4** Dose-response parameters of selective heavy metals

Element	RFD <sup>a</sup> [mg/(kg·d)]	SF <sup>b</sup> (kg·d/mg)
Pb	$3.5 \times 10^{-3}$	-
Ba	$2.0 \times 10^{-1}$	-
Mn	$1.4 \times 10^{-5}$	-
Zn	$3.0 \times 10^{-1}$	-
Cu	$4.0 \times 10^{-2}$	-
As	$3.0 \times 10^{-4}$	15.1
Cr	$2.8 \times 10^{-5}$	8.4

<sup>a</sup>RFD is reference dose

<sup>b</sup>SF is slope factor of cancer risk of elements

**Table 5** Concentrations of elements and their variations in the pre-lockdown and lockdown periods (unit: ng/m<sup>3</sup>)

Element	Pre-lockdown			Lockdown	Rate of descent/%*		
	Strong disturbance	Weak disturbance	Average		No vs strong	No vs week	Week vs strong
Pb	55.8	47.9	51.9	31.5	−43.5	−34.2	−14.2
Se	3.6	3.4	3.5	2.9	−19.4	−14.7	−5.6
Al	2939.5	2642.5	2791.0	2059.2	−29.9	−22.1	−10.1
Si	501.9	564	532.9	385.3	−23.2	−31.7	12.4
As	8.4	5.9	7.2	5.8	−31.0	−1.7	−29.8
Ca	258.4	271.6	265.0	113.2	−56.2	−58.3	5.1
K	697.4	554.4	625.9	632.0	−9.4	14.0	−20.5
Mo	15.7	16.6	16.1	9.8	−37.6	−41.0	5.7
Br	10.3	9.6	9.9	10.2	−1.0	6.3	−6.8
Cr	20.3	31.1	25.7	3.6	−82.3	−88.4	53.2
Zn	128.8	149.7	139.2	31.2	−75.8	−79.2	16.2
Cu	28.6	28.5	28.5	21.6	−24.5	−24.2	−0.3
Fe	351.9	367.4	359.6	127.4	−63.8	−65.3	4.4
Mn	62.1	53.8	57.9	11.1	−82.1	−79.4	−13.4
Ti	91.6	69.6	80.6	13.7	−85.0	−80.3	−24.0
Ba	12.8	13.3	13.0	16.8	31.3	26.3	3.9
Sum	5187.1	4829.3	5008.1	3475.0	−33.0	−28.0	−6.9

\*Descending rate for no vs strong =  $([\text{no disturbance}] - [\text{strong disturbance}]) / [\text{strong disturbance}]$ ; descending rate for no vs weak =  $([\text{no disturbance}] - [\text{weak disturbance}]) / [\text{weak disturbance}]$ ; descending rate for weak vs strong =  $([\text{weak disturbance}] - [\text{strong disturbance}]) / [\text{strong disturbance}]$

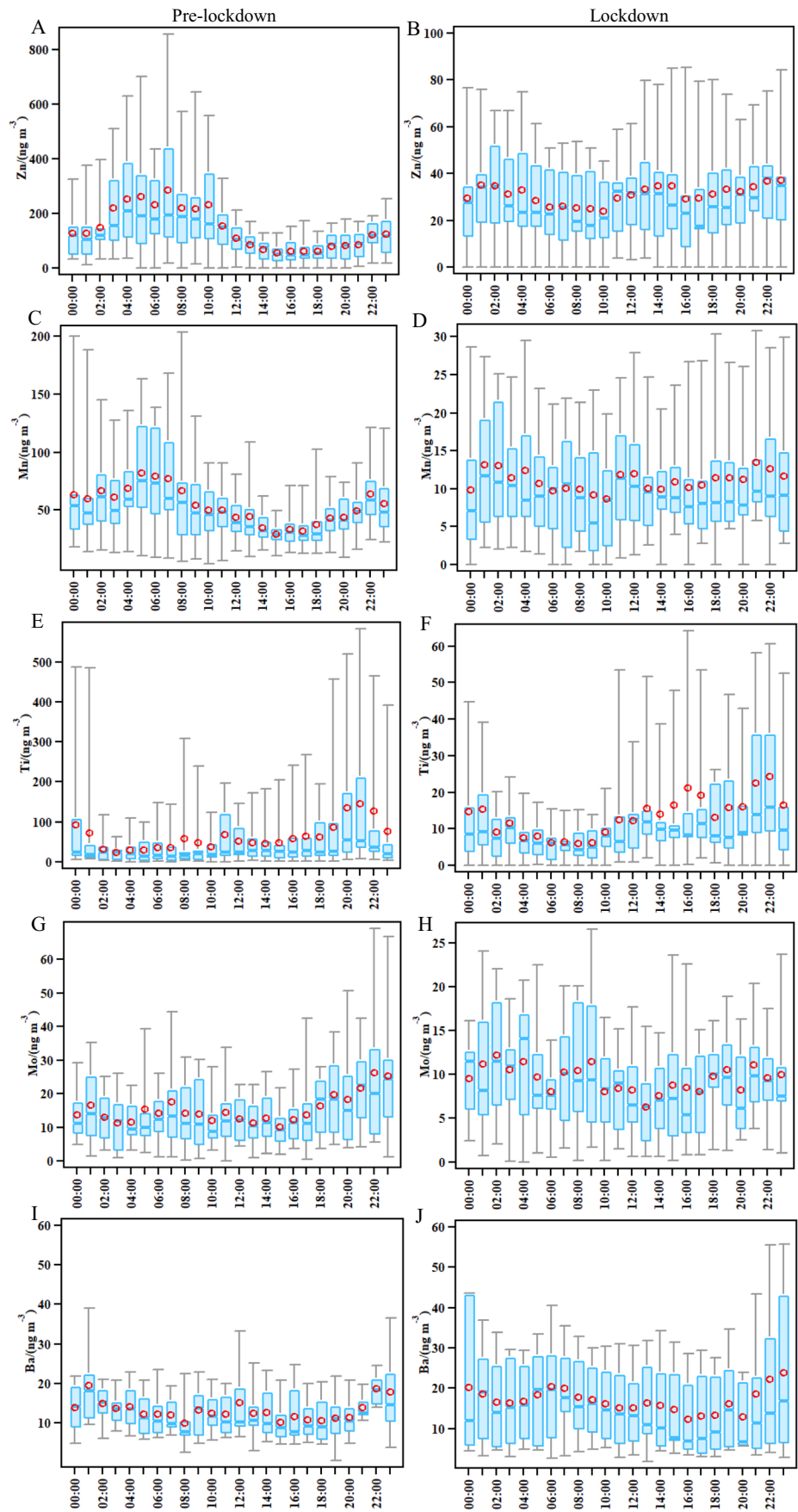
4829 and 5187 ng/m<sup>3</sup>, respectively, which were 28% and 33% higher than that of the lockdown period. The results prove that air pollution control could reduce atmospheric element pollution to a certain extent. To compare the concentration of the lockdown period, the top four elements had the greatest reductions in descending order of Cr (88.4%), Ti (80.3%), Mn (79.4%), and Zn (79.2%) for the strong disturbance scenario; while the sequence was Ti (85.0%), Cr (82.3%), Mn (82.1%), and Zn (75.8%) for the weak disturbance scenario. The findings conclude that the significant contributions of Cr, Ti, Mn, and Zn from the anthropogenic sources in Baoji city on regular days. More specially, Ti and Mn showed larger reductions of 24.0% and 13.4%, respectively, under the weak than the strong anthropogenic disturbance scenarios. However, Cr and Zn showed a reverse trend. Their concentration levels reductions were 53.2% and 16.2%, respectively, higher for the strong than the weak anthropogenic disturbance scenarios. This represents the current pollution measures were more efficiently to control the elements of Ti and Mn.

For other elements, their concentration levels were all higher under the strong than weak anthropogenic disturbances. Under the weak anthropogenic disturbance scenario, the production limit for the electrolytic manganese enterprise is 30% of regular value, while a much lower of 20% is set for the copper smelting processes and furnace productions. The elements of Cu, Al, and other non-ferrous

metals that are used in industrial furnace production must be reduced to 20%. In addition, the limit for Pb smelting furnace production is 30%. The coking enterprises that applied coke oven and blast furnace gases as the main energy sources must be reduced at least 80%, expectedly for the reduced emissions of Se and As. This is consistent with the elaboration in Lu et al. (2009a) that industry emission is the important source of As in Baoji. It should be noted that the elements of Si, Ca, Mo, Cr, Zn, Fe, and Ba under the strong anthropogenic disturbance scenario did not show relatively higher abundances than those of the weak anthropogenic disturbance scenario. These elements are potentially originated from the dusts that long-range transported under favorable meteorological conditions (e.g., wind speed and direction) (Yonemochi et al. 2021). Unfortunately, such natural sources could not be efficiently regulated by any means of control policies. Therefore, it is necessary to consider the origin sources of the elements when a warning signal would be hosted to particular or all industrial sectors for restraining their production during the episode period.

A high score ratio analysis was performed for elements that changed significantly between the two periods. Figure 2 illustrates the time series of selected elements. Compared with the pre-lockdown (139.2 ng/m<sup>3</sup>), the average concentration of Zn decreased exponentially in the lockdown period (31.2 ng/m<sup>3</sup>). The time series showed bi-modal peaks for Zn in the pre-lockdown period, but such the observation

**Fig. 2** High-resolution time series of selective elements during the epidemic in the pre-lockdown (a, c, e, g, i) and lockdown periods (b, d, f, h, j)



was much minor in the lockdown period. The first peak (06:00–08:00 LT) in the morning rush hours could be related to the brake and tire wear of motor vehicles as well as the emissions from zinc smelting and recycling industries. In urban areas, Zn could be more impacted by traffics than the industries (Querol et al. 2007). Another peak was seen at 22:00–02:00 LT when heavy-duty trucks mostly transported goods at nighttime. It is worth noting that the peak value in the daytime ( $285.7 \text{ ng/m}^3$ ) is approximately twice the nighttime ( $125.4 \text{ ng/m}^3$ ), potentially attributed to the traffic flow density.

The variation trends of Mn show a similar bi-modal pattern as Zn. During the pre-lockdown period, the concentration of Mn ranged from 8.10 to  $42.3 \text{ ng/m}^3$ . However, the variation range was comparatively small during the lockdown period. This proves that the atmospheric Mn level was less affected by the emission sources such as traffic, dissimilar to Zn.

The mean concentration of Ti in the pre-lockdown period was  $61.9 \text{ ng/m}^3$  but reduced by 83.0% to  $19.3 \text{ ng/m}^3$  in the lockdown period. The high concentration of Ti occurred at nighttime regularly. The ground temperature on the slopes of the Qinling Mountains declines faster, while the temperature at the bottom of the Qinling Mountains drops more slowly, resulting in great thermal differences and easy formation of mountain winds. The Qinling Mountains are in the south of the sampling site, where the mountain winds could bring the pollutants from the Ti-related industrial parks in the south to the sampling site. In addition, as the solar radiation is reduced at night, air convection is weakened and the atmospheric boundary layer is reduced. These circumstances are non-conductive to the air pollutant diffusion, leading to the accumulation of air pollutants at night. The same observation was also found for the lockdown period. However, due to the control instructions, most industrial enterprises stopped production. Dust might be a more important contributor to Ti.

During the pre-lockdown period, the concentration levels of Mo fluctuated among the daytime but obviously increased at nighttime, consistent with the observations on Ti. It was supposed that Mo from the upwind sites was also affected by the downwind and boundary layer, leading to its accumulation at the downwind sites at night. During the lockdown period, the concentration of Mo comparatively less fluctuated in the daytime, and no obvious peak was shown throughout the whole day. This represents the inactivated industrial activities greatly limited the emissions of Mo to the atmosphere.

The average concentration of Ba in the pre-lockdown period was  $12.8 \text{ ng/m}^3$ , and with a small fluctuation in the daytime. However, during the lockdown period, a higher average concentration of  $16.8 \text{ ng/m}^3$  was seen. As forementioned, Ba is a component emitted from the firework. As the

Spring Festival overlapped with the lockdown period, the traditional household firework activities would be the major source of Ba. It could be further supported by the higher concentration levels were seen at nighttime than daytime during the Spring Festival period.

## Source analysis

PMF model was applied to apportion the sources of elements in  $\text{PM}_{2.5}$  in the two periods of this study. Five major factors were characterized for the pre-lockdown period (Fig. 3), while six factors were identified for the lockdown period (Fig. 4).

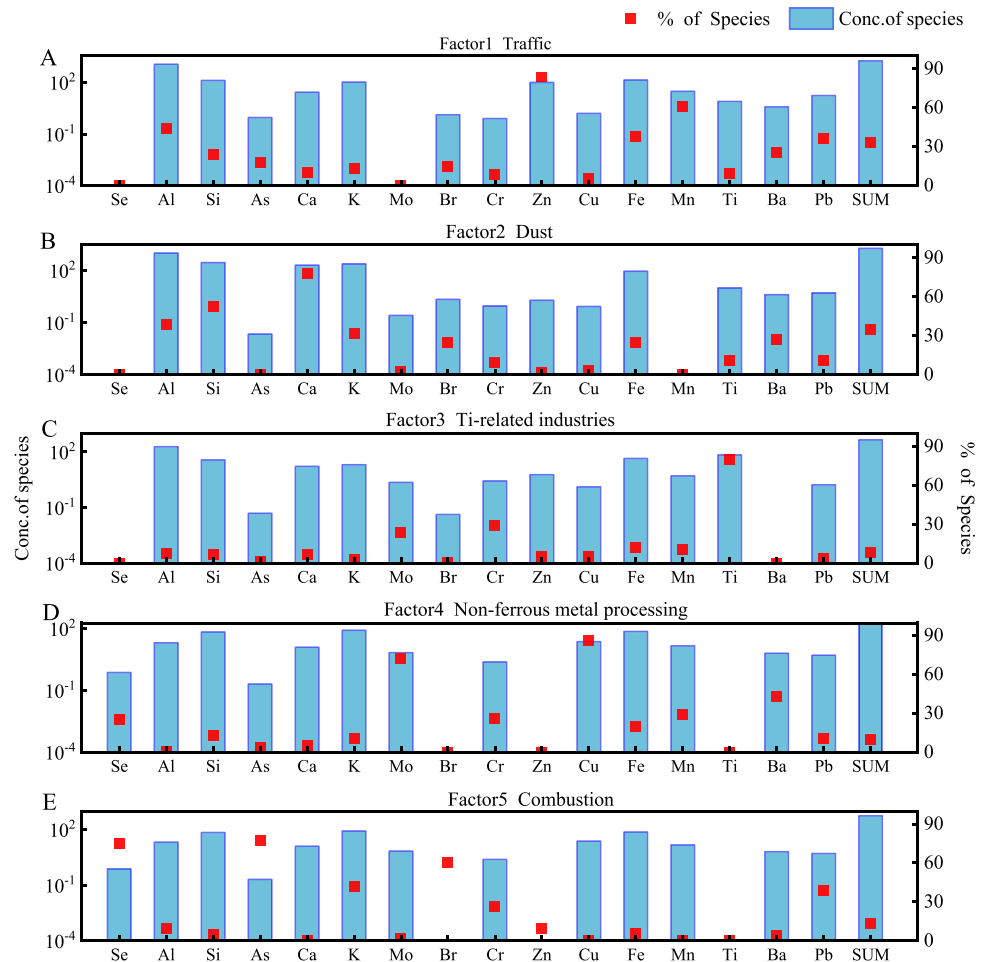
For the pre-lockdown period, the contribution rate of factor 1 is 33.0%, with high loadings of Zn (83.8%), Mn (60.7%), and Al (44.1%), among which Zn is a tracer of traffic emissions (Srimuruganandam and Nagendra 2012). Lu et al. (2009b) also found that Zn concentrations were the highest in places with heavy traffic in Baoji city. Since methylcyclopentadiene manganese tricarbonyl (MMT,  $\text{C}_9\text{H}_7\text{MnO}_3$ ) is usually added to unleaded gasoline to improve engine performance and reduce fuel consumption (Jiao et al. 2019), thus Mn is identified as a tracer for traffic. The wearing process of automobile pistons could produce Al (Kimura et al. 2006). While Al, Si, Fe, and Ca also occupy a certain proportion which may be affected by the ground dusts and the re-suspension during the operation of vehicles. Therefore, factor 1 is identified as the traffic source.

The contribution rate of factor 2 is 35.0%, with the loadings of Ca, Si, Al, and Fe of 78.2%, 52.2%, 38.6%, and 24.7%, respectively. The four elements are the main components of the crust (Viana et al. 2008). Ba also occupies a certain proportion of this factor which may come from dust (Hana et al. 2020). Therefore, it is inferred that this factor is the dust source. However, among them, Fe had the highest decreasing rate (64.6%) from the pre-lockdown to the lockdown periods, while Ca, Si, and Al had relatively small changes, suggesting that Fe was affected by not only dust sources but also possibly from other anthropogenic sources.

The contribution rate of factor 3 is 9.0%, and only element Ti had the characteristic contribution of 79.7%. As forementioned, Baoji is known as the “Titanium Valley of China.” The particles that are produced through the processing of Ti materials should be removed by cyclone and bag technique. However, the efficiencies of cyclone dust removal and the bag dust collector are 85% and 99.5%, respectively. This implies that the Ti-containing particle could not be efficiently eliminated before discharge to the environment. Other elements, including Cr (29.3%), Fe (12.3%), Mn (10.2%), and Si (6.7%), that could change the phase transition temperature of titanium alloy (Wang et al. 2017) also



**Fig. 3 a–e** Source apportionment results from the PMF model in the pre-lockdown period



account for certain proportions. This factor is thus referred to as the Ti-related industries.

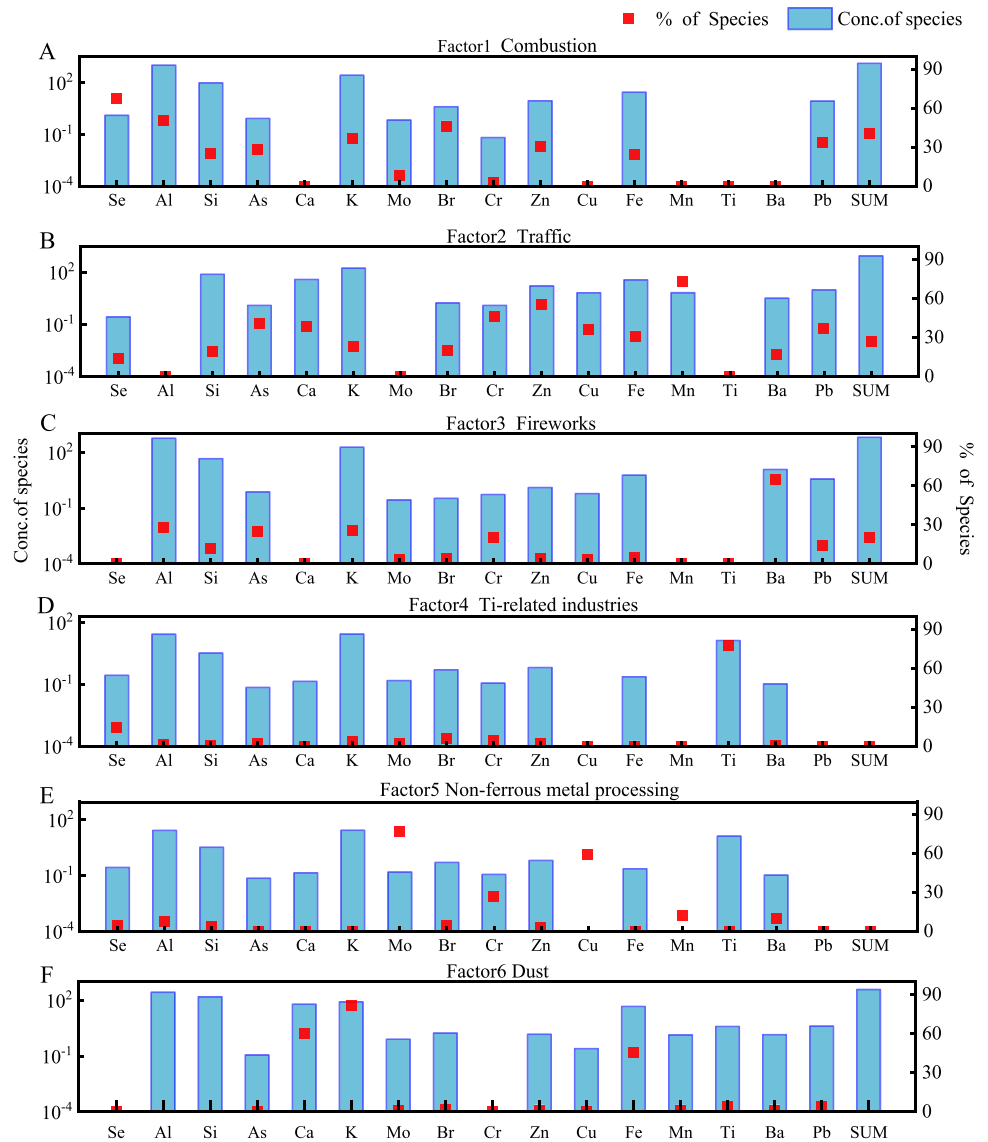
The contribution rate of factor 4 is ~10.0%, with the Cu and Mo loadings of 86.2% and 71.9%, respectively. The Gaojiaya Industrial Park is only 4.5 km away from the sampling point in a straight line. The park mainly consists of non-ferrous metal processing enterprises, and their business scope involved Mo processing. Mo is an alloying element with a higher elastic modulus, higher strength, and better corrosion resistance than Ti (Fan and Ren 2017). The demand for Mo is thus high in Baoji as well. In addition, the porphyry copper-molybdenum deposit is the main source of Mo in China (Lu et al. 2021), so the Cu loading is synchronous high; a previous study (Lu et al. 2010) also found that Cu mainly came from industrial emissions in Baoji. Therefore, it can be inferred that the factor is non-ferrous metal processing.

The contribution rate of factor 5 is 13.0%, among which As (77.4%), Se (74.9%), Br (60.1%), and K (41.7%) had high loadings. Element As is mainly emitted from coal combustion (Hana et al. 2020), Se is originated from the combustion processing (Amil et al. 2016), and K is mainly derived from

biomass combustion (Yu et al. 2018). This factor is thus inferred from the combustion source.

Six factors were resolved for the lockdown period. The contribution rate of factor 1 is 41.0%, among which Se (67.3%), Br (46.2%), and K (36.5%) had high loadings. Hence, it is inferred as the combustion source. The contribution rate of factor 2 is 27.0%; the loadings of Mn and Zn were 73.2% and 55.4%, respectively. It is inferred as the traffic source. The contribution rate of factor 3 is 20.3%, with high loadings of Ba (65.1%), Al (28.2%), K (25.6%), and As (25.0%), respectively. Ba is the tracer of fireworks discharge, while K is the main colorant in fireworks combustion and a component of the fireworks flash effect (Tian et al. 2014). Even the outlier lagged data associated with the discharges from fireworks on January 26 (the Spring Festival) and February 9 (the Lantern Festival) were excluded, the small-scale household fireworks between these days could not be eliminated. Therefore, factor 3 is judged as the source of the fireworks. High Ti loading is seen for factor 4. It is therefore inferred as Ti-related industries. However, the contribution rate of this factor is 0, demonstrating that the Ti-related activities have been substantially affected due to the

**Fig. 4 a–f** Source apportionment results from the PMF model in the lockdown period



lockdown. For factor 5, the loading of Mo and Cu is high. It is inferred to be non-ferrous metal processing. Nevertheless, the contribution rate of this factor is 0 as well, indicating that non-ferrous metal processing enterprises were also shut down in this period. The contribution rate of factor 6 is 12.0%. The loadings of Ca, Si, and Fe are 61.5%, 39.6%, and 39.4%, respectively. This is inferred as the dust source (Table 6).

**Health risk assessment**

The concentrations of different sources were calculated according to the concentration and proportion of elements in each factor resolved in the PMF model (Table 7); the non-carcinogenic risk assessment for the particular elements (i.e., Zn, Mn, Pb, Cr, Cu, Ba, and As) between the two periods

were calculated (Table 8), and the carcinogenic risk assessment was conducted for Cr and As (Table 9).

Based on the limits established by U.S.EPA (1989), HQ less than 1 represents a low non-carcinogenic risk. The threshold of ILCR ranges from 10<sup>-6</sup> to 10<sup>-4</sup> that would suggest potential carcinogenic risk. In terms of threshold, except Mn for traffic, the HQ of other elements are below 1, indicating that their non-carcinogenic risks can be negligible. The ILCR of As that emitted from traffic, combustion, and fireworks, as well as Cr that originated from all sources during the pre-lockdown period, and traffic during the lockdown period were exceed the thresholds, indicating they posed the carcinogenic risk. In terms of population distribution, both values of HQ and ILCR showed descending orders of children > adult male > adult female, consistent with the results of other studies (Zhang et al. 2014). The HQ and ILCR for children are ~ 2.4 and 2.1 times higher than those of adult

**Table 6** Comparison of without and with considerations of meteorological factors on elements during the pre-lockdown and lockdown periods (unit: ng/m<sup>3</sup>)

Elements	Without consideration meteorology		With consideration meteorology	
	Pre-lockdown	Lockdown	Pre-lockdown	Lockdown
Pb	50.7	31.7	51.9	31.5
Se	3.4	2.9	3.5	2.9
Al	2750.5	2113.7	2791.0	2059.2
Si	567.7	418.7	532.9	385.3
As	7.1	5.7	7.2	5.8
Ca	292.2	118.2	265.0	113.2
K	886.7	886.4	625.9	632.0
Mo	16.2	9.8	16.1	9.8
Br	10.1	10.4	9.9	10.2
Cr	22.2	3.4	25.7	3.6
Zn	170.9	35.3	139.2	31.2
Cu	30.1	22.3	28.5	21.6
Fe	378.8	135.3	359.6	127.4
Mn	56.8	13.8	57.9	11.1
Ti	84.6	15.0	80.6	13.7
Ba	17.1	22.5	13.0	16.8

females, indicating that the elements posed a great impact on the health of children.

In terms of types of pollution sources, among the traffic sources, the HQ for Mn associated with traffic to children was greater than 1 in the pre-lockdown period, indicating that traffic posed risks to children. Compared to those in the pre-lockdown period, the HQ of Pb, Zn, Mn, and Cr, and ILCR of Cr decreased in the lockdown period. For the dust sources, the HQ for the related elements showed declines, but the ILCR for As increased after the city lockdown. For the Ti-related industrial sources, Cr had the highest HQ for all age groups. The HQ and ILCR of the elements related to non-ferrous metal processing sources

were significantly reduced with the lockdown policies. The discharges from the fireworks only produced emissions during the lockdown period. As a result, the HQ for Cr, As, Pb, Ba, Cu, and Zn increased while greater ILCR was seen for As than Cr. The ILCR of Cr and the HQ of all elements in the firework could be ignored.

## Conclusions

This study demonstrates the impacts of different degrees of anthropogenic disturbances of industrial activities on the atmospheric elements. Obvious reductions of elements (28–33%) were shown in comparison to those in the lockdown periods. Besides, the warming system showed remarkable benefits to reduce emissions of elements Pb, Se, Al, As, K, Br, Cu, Mn, and Ti in the pre-lockdown period. Dust, traffic sources, combustion, non-ferrous metal processing, and Ti-related industrial processing are the major contributors of the elements to the regular industrial activities in Baoji. The emissions from fireworks for the traditional celebration caused the elevations of the HQ for Zn, Cr, Mn, Pb, Cu, As, and Ba, as well as ILCR for As. The data provides a clear picture of the potential anthropogenic sources of the element in the atmosphere of this typical industrial city.

**Author contribution** Bianhong Zhou, Jin Wang, Qiao Feng, and Chunyan Li: writing—original draft; data curation. Suixin Liu, Tingting Wu, Yong Zhang, Jie Tian, and Steven Sai Hang Ho: writing—review and editing. Qiyuan Wang: supervision.

**Funding** This work was supported by the Key Research and Development Program of Shaanxi Province (2018-ZDXM3-01), the Strategic Priority Research Program of Chinese Academy of Sciences (XDB40000000), the Basic Research Project of Shaanxi Provincial Natural Science (2019JM-120), and the Youth Innovation Promotion Association of the Chinese Academy of Sciences (2019402).

**Table 7** The concentration of elements in different sources (unit: ng/m<sup>3</sup>)

Factor		Pb	As	Zn	Cu	Mn	Ba	Cr
Pre-lockdown	Traffic	18.1	1.1	121.1	1.7	33.9	3.4	2.4
	Dust	5.3	0.0	2.3	0.9	0.0	3.6	2.7
	Ti-related industries	1.8	0.1	7.2	1.4	5.7	0.0	8.3
	Non-ferrous metal processing	5.3	0.3	0.0	24.6	16.2	5.6	7.4
	Combustion	19.4	5.1	13.8	0.0	0.0	0.6	7.5
Lockdown	Traffic	11.6	2.4	17.3	7.8	8.1	5.2	1.6
	Dust	4.9	0.2	1.6	0.3	1.7	2.3	0.0
	Ti-related industries	0.0	0.1	0.7	0.0	0.0	0.2	0.2
	Non-ferrous metal processing	0.0	0.0	0.9	12.8	1.3	3.0	1.0
	Combustion	10.5	1.6	9.4	0.0	0.0	0.0	0.1
Fireworks	4.5	1.5	1.4	0.7	0.0	19.9	0.7	

**Table 8** Health risk assessment for the elements associated with the sources in the pre-lockdown period

		HQ							ILCR		
		Pb	As	Zn	Cu	Mn	Ba	Cr	As	Cr	Cr
Traffic	Child	$2.97 \times 10^{-3}$	$2.18 \times 10^{-3}$	$2.31 \times 10^{-4}$	$2.37 \times 10^{-5}$	$1.39 \times 10^0$	$9.72 \times 10^{-6}$	$4.96 \times 10^{-2}$	$3.29 \times 10^{-6}$	$4.96 \times 10^{-2}$	$3.89 \times 10^{-6}$
	Male	$1.27 \times 10^{-3}$	$9.39 \times 10^{-4}$	$9.96 \times 10^{-5}$	$1.02 \times 10^{-5}$	$5.98 \times 10^{-1}$	$4.18 \times 10^{-6}$	$2.13 \times 10^{-2}$	$1.76 \times 10^{-6}$	$2.13 \times 10^{-2}$	$2.08 \times 10^{-6}$
	Female	$1.22 \times 10^{-3}$	$8.97 \times 10^{-4}$	$9.51 \times 10^{-5}$	$9.72 \times 10^{-6}$	$5.71 \times 10^{-1}$	$3.99 \times 10^{-6}$	$2.04 \times 10^{-2}$	$1.57 \times 10^{-6}$	$2.04 \times 10^{-2}$	$1.86 \times 10^{-6}$
Dust	Child	$8.62 \times 10^{-4}$	$5.12 \times 10^{-5}$	$4.41 \times 10^{-6}$	$1.28 \times 10^{-5}$	—	$1.02 \times 10^{-5}$	$5.63 \times 10^{-2}$	$7.73 \times 10^{-8}$	$5.63 \times 10^{-2}$	$4.41 \times 10^{-6}$
	Male	$3.71 \times 10^{-4}$	$2.20 \times 10^{-5}$	$1.90 \times 10^{-6}$	$5.50 \times 10^{-6}$	—	$4.40 \times 10^{-6}$	$2.42 \times 10^{-2}$	$4.13 \times 10^{-8}$	$2.42 \times 10^{-2}$	$2.36 \times 10^{-6}$
	Female	$3.54 \times 10^{-4}$	$2.10 \times 10^{-5}$	$1.81 \times 10^{-6}$	$5.25 \times 10^{-6}$	—	$4.21 \times 10^{-6}$	$2.31 \times 10^{-2}$	$3.69 \times 10^{-8}$	$2.31 \times 10^{-2}$	$2.11 \times 10^{-6}$
Ti-related industries	Child	$2.89 \times 10^{-4}$	$1.17 \times 10^{-4}$	$1.38 \times 10^{-5}$	$1.98 \times 10^{-5}$	$2.33 \times 10^{-1}$	—	$1.70 \times 10^{-1}$	$1.76 \times 10^{-7}$	$1.70 \times 10^{-1}$	$1.33 \times 10^{-5}$
	Male	$1.25 \times 10^{-4}$	$5.02 \times 10^{-5}$	$5.94 \times 10^{-6}$	$8.50 \times 10^{-6}$	$1.00 \times 10^{-1}$	—	$7.33 \times 10^{-2}$	$9.42 \times 10^{-8}$	$7.33 \times 10^{-2}$	$7.14 \times 10^{-6}$
	Female	$1.19 \times 10^{-4}$	$4.79 \times 10^{-5}$	$5.67 \times 10^{-6}$	$8.12 \times 10^{-6}$	$9.58 \times 10^{-2}$	—	$6.99 \times 10^{-2}$	$8.42 \times 10^{-8}$	$6.99 \times 10^{-2}$	$6.38 \times 10^{-6}$
Non-ferrous metal processing	Child	$8.66 \times 10^{-4}$	$4.82 \times 10^{-4}$	—	$3.52 \times 10^{-4}$	$6.65 \times 10^{-1}$	$1.61 \times 10^{-5}$	$1.51 \times 10^{-1}$	$7.28 \times 10^{-7}$	$1.51 \times 10^{-1}$	$1.18 \times 10^{-5}$
	Male	$3.72 \times 10^{-4}$	$2.08 \times 10^{-4}$	—	$1.52 \times 10^{-4}$	$2.86 \times 10^{-1}$	$6.93 \times 10^{-6}$	$6.49 \times 10^{-2}$	$3.89 \times 10^{-7}$	$6.49 \times 10^{-2}$	$6.33 \times 10^{-6}$
	Female	$3.56 \times 10^{-4}$	$1.98 \times 10^{-4}$	—	$1.45 \times 10^{-4}$	$2.73 \times 10^{-1}$	$6.62 \times 10^{-6}$	$6.21 \times 10^{-2}$	$3.48 \times 10^{-7}$	$6.21 \times 10^{-2}$	$5.66 \times 10^{-6}$
Combustion	Child	$3.18 \times 10^{-3}$	$9.71 \times 10^{-3}$	$2.64 \times 10^{-5}$	—	—	$1.60 \times 10^{-6}$	$1.54 \times 10^{-1}$	$1.47 \times 10^{-5}$	$1.54 \times 10^{-1}$	$1.21 \times 10^{-5}$
	Male	$1.37 \times 10^{-3}$	$4.18 \times 10^{-3}$	$1.14 \times 10^{-5}$	—	—	$6.89 \times 10^{-7}$	$6.62 \times 10^{-2}$	$7.84 \times 10^{-6}$	$6.62 \times 10^{-2}$	$6.45 \times 10^{-6}$
	Female	$1.31 \times 10^{-3}$	$3.99 \times 10^{-3}$	$1.09 \times 10^{-5}$	—	—	$6.58 \times 10^{-7}$	$6.33 \times 10^{-2}$	$7.01 \times 10^{-6}$	$6.33 \times 10^{-2}$	$5.77 \times 10^{-6}$
Average	Child	$8.15 \times 10^{-3}$	$1.10 \times 10^{-3}$	$2.82 \times 10^{-2}$	$4.41 \times 10^{-3}$	$1.04 \times 10^{-2}$	$2.60 \times 10^{-3}$	$5.82 \times 10^{-3}$	$1.94 \times 10^{-5}$	$5.82 \times 10^{-3}$	$5.70 \times 10^{-5}$
	Male	$3.51 \times 10^{-3}$	$4.73 \times 10^{-4}$	$1.21 \times 10^{-2}$	$1.90 \times 10^{-3}$	$4.47 \times 10^{-3}$	$1.12 \times 10^{-3}$	$2.50 \times 10^{-3}$	$1.04 \times 10^{-5}$	$2.50 \times 10^{-3}$	$3.05 \times 10^{-5}$
	Female	$3.35 \times 10^{-3}$	$4.52 \times 10^{-4}$	$1.16 \times 10^{-2}$	$1.81 \times 10^{-3}$	$4.27 \times 10^{-3}$	$1.07 \times 10^{-3}$	$2.40 \times 10^{-3}$	$9.25 \times 10^{-6}$	$2.40 \times 10^{-3}$	$2.72 \times 10^{-5}$

**Table 9** Health risk assessment results for the elements associated with the sources in the lockdown period

		HQ										ILCR		
		Pb	As	Zn	Cu	Mn	Ba	Cr	As	Cr	Cr			
Traffic	Child	$1.90 \times 10^{-3}$	$4.55 \times 10^{-3}$	$3.29 \times 10^{-5}$	$1.12 \times 10^{-4}$	$3.33 \times 10^{-1}$	$1.49 \times 10^{-5}$	$3.36 \times 10^{-2}$	$6.87 \times 10^{-6}$	$3.36 \times 10^{-2}$	$6.87 \times 10^{-6}$	$2.63 \times 10^{-6}$		
	Male	$8.19 \times 10^{-4}$	$1.96 \times 10^{-3}$	$1.42 \times 10^{-5}$	$4.81 \times 10^{-5}$	$1.43 \times 10^{-1}$	$6.42 \times 10^{-6}$	$1.44 \times 10^{-2}$	$3.68 \times 10^{-6}$	$1.44 \times 10^{-2}$	$3.68 \times 10^{-6}$	$1.41 \times 10^{-6}$		
Dust	Female	$7.83 \times 10^{-4}$	$1.87 \times 10^{-3}$	$1.35 \times 10^{-5}$	$4.59 \times 10^{-5}$	$1.37 \times 10^{-1}$	$6.14 \times 10^{-6}$	$1.38 \times 10^{-2}$	$3.28 \times 10^{-6}$	$1.38 \times 10^{-2}$	$3.28 \times 10^{-6}$	$1.26 \times 10^{-6}$		
	Child	$7.98 \times 10^{-4}$	$4.19 \times 10^{-4}$	$2.96 \times 10^{-6}$	$4.21 \times 10^{-6}$	$6.82 \times 10^{-2}$	$6.59 \times 10^{-6}$	—	$6.33 \times 10^{-7}$	—	$6.33 \times 10^{-7}$	—		
	Male	$3.43 \times 10^{-4}$	$1.80 \times 10^{-4}$	$1.27 \times 10^{-6}$	$1.81 \times 10^{-6}$	$2.94 \times 10^{-2}$	$2.83 \times 10^{-6}$	—	$3.39 \times 10^{-7}$	—	$3.39 \times 10^{-7}$	—		
Ti-related industries	Female	$3.28 \times 10^{-4}$	$1.72 \times 10^{-4}$	$1.22 \times 10^{-6}$	$1.73 \times 10^{-6}$	$2.80 \times 10^{-2}$	$2.71 \times 10^{-6}$	—	$3.03 \times 10^{-7}$	—	$3.03 \times 10^{-7}$	—		
	Child	—	$2.64 \times 10^{-4}$	$1.32 \times 10^{-6}$	—	—	$4.94 \times 10^{-7}$	$3.17 \times 10^{-3}$	$3.98 \times 10^{-7}$	$3.17 \times 10^{-3}$	$3.98 \times 10^{-7}$	$2.49 \times 10^{-7}$		
	Male	—	$1.13 \times 10^{-4}$	$5.69 \times 10^{-7}$	—	—	$2.13 \times 10^{-7}$	$1.37 \times 10^{-3}$	$2.13 \times 10^{-7}$	$1.37 \times 10^{-3}$	$2.13 \times 10^{-7}$	$1.33 \times 10^{-7}$		
Non-ferrous metal processing	Female	—	$1.08 \times 10^{-4}$	$5.44 \times 10^{-7}$	—	—	$2.03 \times 10^{-7}$	$1.30 \times 10^{-3}$	$1.90 \times 10^{-7}$	$1.30 \times 10^{-3}$	$1.90 \times 10^{-7}$	$1.19 \times 10^{-7}$		
	Child	—	—	$1.66 \times 10^{-6}$	$1.83 \times 10^{-4}$	$5.37 \times 10^{-2}$	$8.51 \times 10^{-6}$	$1.95 \times 10^{-2}$	—	$1.95 \times 10^{-2}$	—	$1.53 \times 10^{-6}$		
	Male	—	—	$7.13 \times 10^{-7}$	$7.86 \times 10^{-5}$	$2.31 \times 10^{-2}$	$3.66 \times 10^{-6}$	$8.38 \times 10^{-3}$	—	$8.38 \times 10^{-3}$	—	$8.17 \times 10^{-7}$		
Combustion	Female	—	—	$6.81 \times 10^{-7}$	$7.51 \times 10^{-5}$	$2.21 \times 10^{-2}$	$3.49 \times 10^{-6}$	$8.00 \times 10^{-3}$	—	$8.00 \times 10^{-3}$	—	$7.30 \times 10^{-7}$		
	Child	$1.72 \times 10^{-3}$	$3.10 \times 10^{-3}$	$1.80 \times 10^{-5}$	—	—	—	$1.81 \times 10^{-3}$	$4.68 \times 10^{-6}$	$1.81 \times 10^{-3}$	$4.68 \times 10^{-6}$	$1.42 \times 10^{-7}$		
	Male	$7.39 \times 10^{-4}$	$1.33 \times 10^{-3}$	$7.75 \times 10^{-6}$	—	—	—	$7.79 \times 10^{-4}$	$2.50 \times 10^{-6}$	$7.79 \times 10^{-4}$	$2.50 \times 10^{-6}$	$7.59 \times 10^{-8}$		
Fireworks	Female	$7.06 \times 10^{-4}$	$1.27 \times 10^{-3}$	$7.39 \times 10^{-6}$	—	—	—	$7.45 \times 10^{-4}$	$2.24 \times 10^{-6}$	$7.45 \times 10^{-4}$	$2.24 \times 10^{-6}$	$6.79 \times 10^{-8}$		
	Child	$7.34 \times 10^{-4}$	$2.78 \times 10^{-3}$	$2.62 \times 10^{-6}$	$1.04 \times 10^{-5}$	—	$5.70 \times 10^{-5}$	$1.50 \times 10^{-2}$	$4.20 \times 10^{-6}$	$1.50 \times 10^{-2}$	$4.20 \times 10^{-6}$	$1.17 \times 10^{-6}$		
	Male	$3.16 \times 10^{-4}$	$1.20 \times 10^{-3}$	$1.13 \times 10^{-6}$	$4.47 \times 10^{-6}$	—	$2.45 \times 10^{-5}$	$6.44 \times 10^{-3}$	$2.25 \times 10^{-6}$	$6.44 \times 10^{-3}$	$2.25 \times 10^{-6}$	$6.28 \times 10^{-7}$		
Average	Female	$3.02 \times 10^{-4}$	$1.14 \times 10^{-3}$	$1.08 \times 10^{-6}$	$4.27 \times 10^{-6}$	—	$2.34 \times 10^{-5}$	$6.15 \times 10^{-3}$	$2.01 \times 10^{-6}$	$6.15 \times 10^{-3}$	$2.01 \times 10^{-6}$	$5.61 \times 10^{-7}$		
	Child	$4.87 \times 10^{-3}$	$9.12 \times 10^{-4}$	$5.56 \times 10^{-3}$	$3.06 \times 10^{-3}$	$1.81 \times 10^{-3}$	$3.20 \times 10^{-3}$	$4.90 \times 10^{-4}$	$1.61 \times 10^{-5}$	$4.90 \times 10^{-4}$	$1.61 \times 10^{-5}$	$4.81 \times 10^{-6}$		
	Male	$2.09 \times 10^{-3}$	$3.92 \times 10^{-4}$	$2.40 \times 10^{-3}$	$1.31 \times 10^{-3}$	$7.79 \times 10^{-4}$	$1.38 \times 10^{-3}$	$2.11 \times 10^{-4}$	$8.60 \times 10^{-6}$	$2.11 \times 10^{-4}$	$8.60 \times 10^{-6}$	$2.57 \times 10^{-6}$		
	Female	$2.00 \times 10^{-3}$	$3.75 \times 10^{-4}$	$2.29 \times 10^{-3}$	$1.26 \times 10^{-3}$	$7.44 \times 10^{-4}$	$1.32 \times 10^{-3}$	$2.02 \times 10^{-4}$	$7.68 \times 10^{-6}$	$2.02 \times 10^{-4}$	$7.68 \times 10^{-6}$	$2.30 \times 10^{-6}$		

**Data availability** The data used in this manuscript is included in the text.

## Declarations

**Ethics approval and consent to participate** Not applicable.

**Consent for publication** Not applicable.

**Competing interests** The authors declare no competing interests.

## References

- Amil N, Latif MT, Khan MF, Mohamad M (2016) Seasonal variability of PM<sub>2.5</sub> composition and sources in the Klang Valley urban-industrial environment. *Atmos. Chem Phys* 16(8):5357–5381. <https://doi.org/10.5194/acp-16-5357-2016>
- Chang YH, Huang K, Xie MJ, Deng CR, Zou Z, Liu SD, Zhang YL (2018) First long-term and near real-time measurement of trace elements in China's urban atmosphere: temporal variability, source apportionment and precipitation effect. *Atmos Chem Phys* 18(16):11793–11812. <https://doi.org/10.5194/acp-18-11793-2018>
- Dai QL, Liu BS, Bi XH, Wu JH, Liang DN, Zhang YF, Feng YC, Hopke PK (2020) Dispersion normalized PMF provides insights into the significant changes in source contributions to PM<sub>2.5</sub> after the COVID-19 outbreak. *Environ Sci Technol* 54(16):9917–9927. <https://doi.org/10.1021/acs.est.0c02776>
- Fan XP, Ren XQ (2017) Influence of Mo content on microstructure and properties of Ti-Mo alloy. *Hot Work Technol* 46(6):46–48. <https://doi.org/10.14158/j.cnki.1001-3814.2017.06.013>
- Han YJ, Kim HW, Cho SH, Kim PR, Kim WJ (2015) Metallic elements in PM<sub>2.5</sub> in different functional areas of Korea: concentrations and source identification. *Atmos Res* 153:416–428. <https://doi.org/10.1016/j.atmosres.2014.10.002>
- Hana C, Pavel M, Jitka H, Petra P, Jaroslav S, Jozef K (2020) Seasonal variation and sources of elements in urban submicron and fine aerosol in Brno, Czech Republic. *Aerosol Air Qual Res* 21:1–19+ap1. <https://doi.org/10.4209/aaqr.2020.09.0556>
- Hao YF, Meng XP, Yu XP, Lei ML, Li WJ, Shi FT, Yang WW, Zhang SJ, Xie SD (2018) Characteristics of trace elements in PM<sub>2.5</sub> and PM<sub>10</sub> of Chifeng, northeast China: insights into spatiotemporal variations and sources. *Atmos Res* 213:550–561. <https://doi.org/10.1016/j.atmosres.2018.07.006>
- Hwang SL, Chi MC, Guo SE, Lin YC, Chou CT, Lin CM (2018) Seasonal variation and source apportionment of PM<sub>2.5</sub>-bound trace elements at a coastal area in southwestern Taiwan. *Environ Sci Pollut Res Int* 25(9):9101–9113. <https://doi.org/10.1007/s11356-017-1144-2>
- Jiao P, Zhang J, Lv J, Yu N (2019) Refined pretreatment process of gasoline antiknock agent methylcyclopentadienyl manganese tricarbonyl (MMT) product involves removing solid insoluble matter by solid-liquid separation of MMT synthesis reaction solution and distilling. CN109438524-A, China
- Kimura K, Lynskey M, Corrigan ER, Hickman DL, Chatterjee S (2006) Real world study of diesel particulate filter ash accumulation in heavy-duty diesel trucks. *Soc Automot Eng Tech Pap Ser* 33. <https://doi.org/10.4271/2006-01-3257>
- Li C (2021) Study on the current situation and countermeasures of industrial pollution control in Baoji. Xinjiang University, Xinjiang, pp 11–15. <https://doi.org/10.27429/d.cnki.gxjdu.2020.000221>
- Liu G, Li JH, Wu D, Xu H (2015) Chemical composition and source apportionment of the ambient PM<sub>2.5</sub> in Hangzhou. *China Particology* 18:135–143. <https://doi.org/10.1016/j.partic.2014.03.011>
- Lu XW, Li LY, Wang LJ, Lei K, Huang J, Zhang YX (2009a) Contamination assessment of mercury and arsenic in roadway dust from Baoji, China. *Atmos Environ* 43(15):2489–2496. <https://doi.org/10.1016/j.atmosenv.2009.01.048>
- Lu XW, Wang LJ, Lei K, Huang J, Zhang YX (2009b) Contamination assessment of copper, lead, zinc, manganese and nickel in street dust of Baoji, NW China. *J Hazard Mater* 161:1058–1062. <https://doi.org/10.1016/j.jhazmat.2008.04.052>
- Lu XW, Wang LJ, Li LY, Lei K, Huang L, Kang D (2010) Multivariate statistical analysis of heavy metals in street dust of Baoji, NW China. *J Hazard Mater* 173:744–749. <https://doi.org/10.1016/j.jhazmat.2009.09.001>
- Lu T, Yuan ZT, Song K, Tong JC, Zhang HH (2021) Separation test study on the combined process of magnetic separation and flotation for copper and molybdenum mixed concentrate. *Metal Mine* 9:85–90. <https://doi.org/10.19614/j.cnki.jsks.202109012>
- Manousakas M, Papaefthymiou H, Diapouli E, Migliori A, Karydas AG, Bogdanovic-Radovic I, Eleftheriadis K (2017) Assessment of PM<sub>2.5</sub> sources and their corresponding level of uncertainty in a coastal urban area using EPA PMF 5.0 enhanced diagnostics. *Sci Total Environ* 574:155–164. <https://doi.org/10.1016/j.scitotenv.2016.09.047>
- Mishra AK, Rajput P, Singh A, Singh CK, Mall RK (2021) Effect of lockdown amid COVID-19 on ambient air quality in 16 Indian cities. *Front Sustain Cit*. <https://doi.org/10.3389/frsc.2021.705051>
- Nguyen TPM, Bui TH, Nguyen MK, Nguyen TH, Vu VT, Pham HL (2021) Impact of Covid-19 partial lockdown on PM<sub>2.5</sub>, SO<sub>2</sub>, NO<sub>2</sub>, O<sub>3</sub>, and trace elements in PM<sub>2.5</sub> in Hanoi, Vietnam. *Environ Sci Pollut Res*. <https://doi.org/10.1007/s11356-021-13792-y>
- Paatero P, Tapper U (1994) Positive matrix factorization: a non-negative factor model with optimal utilization of error estimates of data values. *Environmetrics* 5:111–126. <https://doi.org/10.1002/env.3170050203>
- Querol X, Viana M, Alastuey A, Amato F, Moreno T, Castillo S, Pey J, de la Rosa J, Sánchez de la Campa A, Artíñano B, Salvador P, García Dos Santos S, Fernández-Patier R, Moreno-Grau S, Negral L, Minguillón MC, Monfort E, Gil JI, Inza A et al (2007) Source origin of trace elements in PM from regional background, urban and industrial sites of Spain. *Atmos Environ* 41(34):7219–7231. <https://doi.org/10.1016/j.atmosenv.2007.05.022>
- Rai P, Furger M, Slowik J, Canonaco F (2020) Source apportionment of highly time resolved trace elements during a firework episode from a rural freeway site in Switzerland. *Atmos Chem Phys* 20(3):1657–1674. <https://doi.org/10.5194/acp-2018-1229>
- Shah MH, Shaheen N, Nazir R (2012) Assessment of the trace elements level in urban atmospheric particulate matter and source apportionment in Islamabad, Pakistan. *Atmos Pollut Res* 3(1):39–45. <https://doi.org/10.5094/APR.2012.003>
- Sorensen M, Schins RPF, Hertel O, Loft S (2005) Transition metals in personal samples of PM<sub>2.5</sub> and oxidative stress in human volunteers. *Cancer Epidemiol Biomark Prev* 14(5):1340–1343. <https://doi.org/10.1088/0143-0807/27/2/010>
- Srimuruganandam B, Nagendra SMS (2012) Source characterization of PM<sub>10</sub> and PM<sub>2.5</sub> mass using a chemical mass balance model at urban roadside. *Sci Total Environ* 433:8–19. <https://doi.org/10.1016/j.scitotenv.2012.05.082>
- Tenías JM, Ballester F, Perez-Hoyos S, Rivera ML (2010) Air pollution and hospital emergency room admissions for chronic obstructive pulmonary disease in Valencia, Spain. *Arch Environ Health* 57(1):41–47. <https://doi.org/10.1080/00039890209602915>
- The Ministry of Environmental Protection (2013) Handbook of Exposure Parameters for the Chinese population-adult volume. China Environmental Science Press, Beijing, pp 271–280

- Thomas LDK, Hodgson S, Nieuwenhuijsen M, Jarup L (2009) Early kidney damage in a population exposed to cadmium and other heavy metals. *Environ Health Perspect* 117:181–184. <https://doi.org/10.1289/ehp.11641>
- Tian YZ, Wang J, Peng X, Shi GL, Feng YC (2014) Estimation of the direct and indirect impacts of fireworks on the physicochemical characteristics of atmospheric PM<sub>10</sub> and PM<sub>2.5</sub>. *Atmos. Chem Phys* 14(18):9469–9479. <https://doi.org/10.5194/acp-14-9469-2014>
- United States Environmental Protection Agency (1989) Risk assessment guidance for superfund. Volume I: Human Health Evaluation Manual Supplemental Guidance
- Viana M, Kuhlbusch TAJ, Querol X, Alastuey A, Harrison RM, Hopke PK, Winiwarter W, Vallius M, Szidat S, Prévôt ASH, Hueglin C, Bloemen H, Wählin P, Vecchi R, Miranda AI, Kasper-Giebl A, Maenhaut W, Hittenberger R (2008) Source apportionment of particulate matter in Europe: a review of methods and results. *J Aerosol Sci* 39(10):827–849. <https://doi.org/10.1016/j.jaerosci.2008.05.007>
- Wang SM, Bai XF, Zhu B, Xia JH, Wang T, Ma XC, Ma Y (2017) Discussion on the transformation point of titanium alloy. *J Xi'an Univ (Natural Science Edition)* 20:92–96. <https://doi.org/10.3969/j.issn.1008-5564.2017.04.021>
- Wang SB, Yu X, Zhao QY, Yang LM, Yin SS, Zhang RQ (2018) Analysis of the formation of two typical atmospheric heavy pollution episodes in Zhengzhou, China. *China. Environ Sci* 38(7):2425–2431. <https://doi.org/10.19674/j.cnki.issn1000-6923.2018.0248>
- Wang YC, Yuan Y, Wang QY, Liu CG, Zhi Q, Cao JJ (2020) Changes in air quality related to the control of coronavirus in China: implications for traffic and industrial emissions. *Sci Total Environ* 731:139133. <https://doi.org/10.1016/j.scitotenv.2020.139133>
- Yao L, Wang DF, Fu QY, Qiao LP, Wang HL, Li L, Sun WW, Li Q, Wang L, Yang X, Zhao ZH, Kan HD, Xian AY, Wang GH, Xiao H, Chen JM (2019) The effects of firework regulation on air quality and public health during the Chinese Spring Festival from 2013 to 2017 in a Chinese megacity. *Environ Int* 126:96–106. <https://doi.org/10.1016/j.envint.2019.01.037>
- Yin HM, Chen JH, Feng XQ, Xu XM, Jiang T, Qian J, Ye H (2019) Pollution characteristics and source analysis of carbonaceous aerosol in PM<sub>2.5</sub> in Yibin, China. *Environ Chem* 38:738–745. <https://doi.org/10.7524/j.issn.0254-6108.2018061504>
- Yonemochi S, Hori Y, Konishi T, Lee KH, Kim YJ, Hatakeyama S, Okochi H (2021) Clarification of emission source by inorganic elements in PM<sub>2.5</sub> collected in the daytime and night at the top of Mt. Fuji *Bunseki Kagaku* 70(6):363–371. <https://doi.org/10.2116/bunsekikagaku.70.363>
- Yu JT, Yan CQ, Liu Y, Li XM, Zhou T, Zheng M (2018) Potassium: a tracer for biomass burning in Beijing? *Aerosol Air Qual Res* 18(9):2447–2459. <https://doi.org/10.4209/aaqr.2017.11.0536>
- Zhang Q (2004) Characteristics and strategy innovation of baoji industrialization process. *J Baoji Univ Arts Sci (Soc Sci)* 34(1):63–67. <https://doi.org/10.13467/j.cnki.jbuss.2014.01.012>
- Zhang M (2007) Modern industry of Baoji during the anti-Japanese war. *J Xi'an Polytech Univ* 2:253–256. <https://doi.org/10.3969/j.issn.1674-649X.2007.02.027>
- Zhang YF, Xu H, Liu GR, Tian YZ, Shi GL, Wu JH, Zhang P, Zhou LD, Feng YC (2014) Evaluation of the changes of the concentration, composition and possible sources of size-resolved particulate matter between 2010 and 2011 in a Western Chinese Mega City. *Aerosol Air Qual Res* 14(5):1500–1514. <https://doi.org/10.4209/aaqr.2013.04.0108>
- Zhang WH, Peng X, Bi XH, Cheng Y, Liang DN, Wu JH, Tian YZ, Zhang YF, Feng YC (2021) Source apportionment of PM<sub>2.5</sub> using online and offline measurements of chemical components in Tianjin, China. *Atmos Environ* 244:117942. <https://doi.org/10.1016/j.atmosenv.2020.117942>
- Zhou BH, Wang J, Cao X, Zhang R, Liu Y, Xu DD (2020) Characteristics and health risk assessments of elements in PM<sub>2.5</sub> during winter in Baoji City. *Asian J Ecotoxicol* 15:299–311. <https://doi.org/10.7524/AJE.1673-5897.20200407001>

**Publisher's note** Springer Nature remains neutral with regard to jurisdictional claims in published maps and institutional affiliations.